

Distributed Learning of Neural Networks using Independent Subnet Training

Binhang Yuan
Rice University
by8@rice.edu

Cameron R. Wolfe
Rice University
crw13@rice.edu

Chen Dun
Rice University
cd46@rice.edu

Yuxin Tang
Rice University
yuxin.tang@rice.edu

Anastasios Kyrillidis
Rice University
anastasios@rice.edu

Chris Jermaine
Rice University
cmj4@rice.edu

ABSTRACT

Distributed machine learning (ML) can bring more computational resources to bear than single-machine learning, reducing training time. Further, distribution allows models to be partitioned over many machines, allowing very large models to be trained—models that may be much larger than the available memory of any individual machine. However, in practice, distributed ML remains challenging, primarily due to high communication costs. We propose a new approach to distributed neural network learning, called independent subnet training (IST). In IST, per iteration, a neural network is decomposed into a set of subnetworks of the same depth as the original network, each of which is trained locally, before the various subnets are exchanged and the process is repeated. IST training has many advantages over standard data parallel approaches. Because the original network is decomposed into independent parts, communication volume is reduced. The decomposition makes IST naturally “model parallel”, and so IST scales to very large models that cannot fit on any single machine. Furthermore, because the subsets are independent, communication frequency is reduced. We show experimentally that IST results in training times that are much lower than data parallel approaches to distributed learning. Furthermore, IST scales to large models that cannot be learned using standard approaches.

1 INTRODUCTION

Distributed neural network (NN) training over a compute cluster has become an essential task in modern computing systems [12, 15, 25, 36, 44]. Distributed training algorithms may be roughly categorized into *model parallel* and *data parallel*. In the former [15, 25], different compute nodes are responsible for different parts of a NN. In the latter [21, 43, 67], each compute node updates a complete copy of the NN’s parameters on different data. In both cases, the obvious way to speed up learning is to add more nodes. With more hardware, the model is split across more CPUs/GPUs in the model parallel setting, or gradients are computed using fewer data objects per compute node in the data parallel setting.

Due to its ease-of-implementation, data parallel training is most commonly used, and it is better supported by common deep learning software, such as TensorFlow [2] and PyTorch [42]. However, there are limitations preventing data parallelism from easily scaling out. Adding nodes means that each node can perform forward and backward propagation more quickly on its own local data, but it leaves the synchronization step no faster. In fact, if synchronization

time dominates, adding more machines could actually make training even *slower* as the number of bytes transferred to broadcast an updated model grows linearly with cluster size. This is particularly problematic in public clouds, such as Amazon EC2¹, that tend to couple relatively slow interconnects with high-performance GPUs, meaning that transfer costs dominate. One can increase batch size to decrease the relative cost of the synchronization step, but this can introduce statistical inefficiency. While there is some debate about the utility of large-batch methods in practice [22, 38], very large batch sizes often do not speed up convergence unless special configuration and tuning is performed, and large batches can also hurt generalizability [13, 23, 50, 58, 60–62].

Independent subnet training. The central idea in this paper, called *independent subnet training* (IST), facilitates combined model and data parallel distributed training. IST utilizes ideas from dropout [51] and approximate matrix multiplication [19]. IST decomposes the NN layers into a set of *subnets* for the same task, by partitioning the neurons across different sites. Each of those subnets is trained for one or more local stochastic gradient descent (SGD) iterations, before synchronization.

Since subnets share no parameters in the distributed setting, synchronization requires no aggregation on these parameters, in contrast to the data parallel method—it is just an exchange of parameters. Moreover, because subnets are sampled without replacement, the interdependence among them is minimized, which allows their local SGD updates for a larger number of iterations without significant “model drifting”, before synchronizing. This reduces communication frequency. Communication costs per synchronization step are also reduced because in an n -machine cluster, each machine gets between $\frac{1}{n^2}$ and $\frac{1}{n}$ of the weights—contrast this to data parallel training, when each machine must receive *all* of the weights.

IST has advantages over model parallel approaches. Since subnets are trained independently during local updates, no synchronization between subnetworks is required. Yet, IST inherits the advantages of model parallel methods. Since each machine gets just a small fraction of the overall model, IST allows the training of very large models that cannot fit into the RAM of a node or a device. This can be an advantage when training large models using GPUs, which tend to have limited memory.

¹89% of cloud-based deep learning projects are executed on EC2, according to Amazon’s marketing materials.

Our Contributions. This paper has the following key contributions.

- We propose independent subnet training, a method for combined model parallel/data parallel training of neural networks on a cluster of machines. IST is specifically designed to work well on public clouds, where it is difficult to realize high-performance, distributed training. These clouds often combine high performance CPUs and GPUs with relatively low-speed inter-machine interconnects.
- We evaluate IST on speech recognition, image classification (CIFAR10 and full ImageNet), and a large-scale Amazon product recommendation task. We find that IST results in up to a 10× speedup for time-to-convergence, compared to a state-of-the-art data parallel realization, using bandwidth-optimal ring all-reduce [1], as well as the “vanilla” local SGD method [37].
- Because IST allows for efficient implicit model parallel training, we show that IST can solve an “extreme” Amazon product recommendation task with improved generalization, by increasing the embedding dimensions for larger models, which is not supported by data parallel based training.
- Finally, we present theoretical results showing that decomposing a neural network into subnets for distributed training still allows for convergence under a set of standard assumptions.

2 PRELIMINARIES

NN training. We are interested in optimizing a loss function $\ell(\cdot, \cdot)$ over a set of labeled examples; the loss $\ell(w, \cdot)$ encodes the NN architecture, with parameters w . Given samples $X := \{x_i, y_i\}_{i=1}^n$, deep learning aims in finding w^* that minimizes the *empirical loss*:

$$w^* \in \arg \min_w \frac{1}{n} \sum_{i=1}^n \ell(w, \{x_i, y_i\}). \quad (1)$$

Formula (1) is completed using various approaches [20, 33, 46, 56, 63], but almost all NN training is accomplished via some variation on SGD: we compute (stochastic) gradient directions $\nabla \ell_i(w_i) := \nabla \ell(w_i, \{x_i, y_i\})$ that, on expectation, decrease the loss, and then set $w_{t+1} \leftarrow w_t - \eta \nabla \ell_i(w_t)$. Here, $\eta > 0$ is the learning rate, and i_t represents a mini-batch of examples, selected from X .

Why classical distributed approaches can be ineffective? Computing $\nabla \ell(w_t, X)$ over the whole X is wasteful [16]. Instead, mini batch SGD computes $w_{t+1} \leftarrow w_t - \eta \nabla \ell(w_t, X_{i_t})$ for a small subsample X_{i_t} of X . In a centralized system, we often use no more than a few hundred data items in X_{i_t} , and few would advocate using more than a few tens of thousands of X_{i_t} [23, 50, 58].

For distributed computation, this is problematic for two reasons: first, it makes it difficult to speed up the computation by adding more computing hardware. Since the batch size $|X_{i_t}|$ is small, splitting the task to more than a few compute nodes is not beneficial, which motivates different training approaches for NNs [6, 7, 9, 35, 39, 57]. Second, gathering the updates in a distributed setting introduces a non-negligible time overhead in large clusters, which is often the main bottleneck towards efficient large-scale computing — see Section 5. This imbalance between communication and computation capacity may lead to significant *increases* in training time when a larger cluster is used.

3 TRAINING VIA INDEPENDENT SUBNETS

Assume n sites in a distributed system. For simplicity, we assume all layers of the NN utilize the same activation function. Let f^l denote that vector of activations at layer l . f^l denotes the set of activations at the final or “top” layer of the network, and f^0 denotes the feature vector that is input into the network. Assume that the number of neurons at layer l is N_l . IST is a randomized, distributed training regime that utilizes a set of *membership indicators*:

$$\{m_{s,i}^l\}_{s \in \{1, \dots, n\}, i \in \{1, \dots, N_l\}}$$

Here, s ranges over the n sites, and i ranges over the neurons in layer l . Each $m_{s,i}^l \in \{0, 1\}$, is randomly selected, where the marginal probability is $\mathbb{P}[m_{s,i}^l = 1] = \frac{1}{n}$. Further, for each layer l and activation i , we constrain $\sum_s m_{s,i}^l$ to be 1 and the covariance of $m_{s,i}^l$ and $m_{s,i'}^{l-1}$ must be zero, so that $\mathbb{E}[m_{s,i}^l m_{s,i'}^{l-1}] = \frac{1}{n^2}$.

Then, we define the recurrence at the heart of IST:

$$\hat{f}^l = f \left(n^2 \sum_s m_s^l \odot \left(W^l \left(m_s^{l-1} \odot \hat{f}^{l-1} \right) \right) \right). \quad (2)$$

Here, W^l is the weight matrix connecting layer $l-1$ and layer l , and \odot denotes the Hadamard product of the two vectors. This recurrence is useful for two key reasons. First, it is easy to argue that if \hat{f}^{l-1} is an unbiased estimator for f^{l-1} , then $n^2 \sum_s m_s^l \odot \left(W^l \left(m_s^{l-1} \odot \hat{f}^{l-1} \right) \right)$, is an unbiased estimator for $W^l f^{l-1}$. To show this, we note that the j th entry in the vector $n^2 \sum_s m_s^l \odot \left(W^l \left(m_s^{l-1} \odot \hat{f}^{l-1} \right) \right)$ is computed as $n^2 \sum_s \sum_i \sum_{i'} W_{j,i}^l m_{s,i}^l m_{s,i'}^{l-1} \hat{f}_i^{l-1}$, and hence its expectation is:

$$\begin{aligned} & \mathbb{E} \left[n^2 \sum_s \sum_i \sum_{i'} W_{j,i}^l m_{s,i}^l m_{s,i'}^{l-1} \hat{f}_i^{l-1} \right] \\ &= n^2 \sum_s \sum_i \sum_{i'} W_{j,i}^l \mathbb{E} \left[m_{s,i}^l m_{s,i'}^{l-1} \hat{f}_i^{l-1} \right] \\ &= n^2 \sum_s \sum_i \frac{1}{n^2} W_{j,i}^l \mathbb{E} \left[\hat{f}_i^{l-1} \right] \\ &= \sum_i W_{j,i}^l f_i^{l-1} \end{aligned}$$

which is precisely the j th entry in $W^l f^{l-1}$.

This unbiasedness suggests that this recurrence can be computed in place of the standard recurrence implemented by a NN, $f^l = f \left(W^l f^{l-1} \right)$. A feature vector can be pushed through the resulting “approximate” NN, and the final vector \hat{f}^l can be used as an approximation for f^l .

3.1 Distributing Independent Subnets

The second reason the recurrence is useful is that it is much easier to distribute the computation of \hat{f}^l —and its backpropagation—than that of f^l . When randomly generating $\{m_{s,i}^l\}_{s \in \{1, \dots, n\}, i \in \{1, \dots, N_l\}}$, we require that $\sum_s m_{s,i}^l$ be 1. Two important aspects follow directly from this requirement. First, in the summation of Formula (2), only one “site” can contribute to the j th entry in the vector \hat{f}^l ; this is due to the Hadamard product with m_s^l , which implies that all other sites’ contributions will be zeroed out. Second, only the entries in \hat{f}^{l-1} that were *themselves* associated with the same site value for s

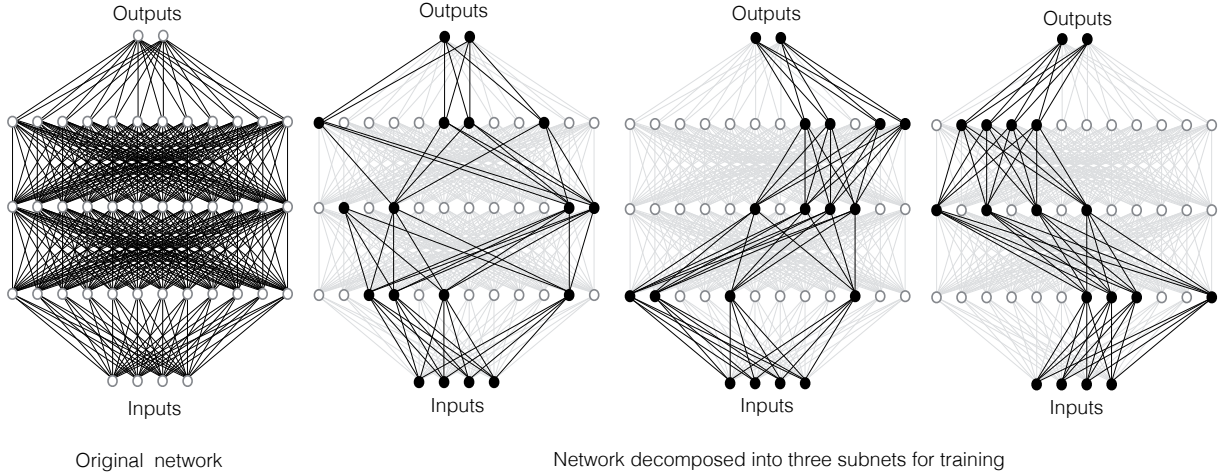


Figure 1: Decomposing a NN with three hidden layers into three subnets.

can contribute to the j th entry, again due to the Hadamard product with m_s^{l-1} .

This implies that we can co-locate at site s the computation of all entries in \hat{f}^{l-1} where $m_{s,i}^{l-1}$ is 1, and all entries in \hat{f}^l where $m_{s,i}^l$ is 1. No cross-site communication is required to compute the activations in layer l from the activations in layer $l-1$. Further, since only the entries in W_j for which $m_{s,i}^l m_{s,i}^{l-1} = 1$ are used at site i —and on expectation, only $\frac{1}{n^2}$ of the weights in W^l will be used—this implies that during an iteration of distributed backpropagation, each site needs only (and communicates gradients for) a fraction $\frac{1}{n^2}$ of the weights in each weight matrix.

The distributed implementation of the recurrence across three sites for a feedforward NN with three hidden layers is depicted in Figure 1. The convolutional NN case is described later in the text. The neurons in each layer are partitioned randomly across the sites, except for the input layer, which is fully utilized at all sites and the output layer, which computes all of the activations at the top layer.

3.2 Distributed Training Algorithm

This suggests an algorithm for distributed learning, given in Algorithm 1 and Algorithm 2. Algorithm 1 repeatedly samples a set of membership indicators, and then partitions the model weights across the set of compute nodes. Since the weights are fully partitioned, the independent subsets can be trained separately on local data for a number of iterations (Algorithm 2), before the indicators are re-sampled, and the weights are re-shuffled across the nodes. Note that periodic resampling of the indicators (followed by reshuffling) is necessary due to the possible accumulation of random effects. While the recurrence of eq. (2) provides for an unbiased estimate for the input to a neuron, after backpropagation, the expected input to a neuron will change. Since each subset is being trained using samples from the same data distribution, this shift may be inconsistent across sites. Resampling guards against this.

3.3 Correcting Distributional Shift

There is, however, a significant problem with the above formulation. Specifically, by eq. (2), we argued that $n^2 \sum_s m_s^l \odot (W^l (m_s^{l-1} \odot \hat{f}^{l-1}))$

Algorithm 1 Independent subnet training.

```

1: Initialize weight matrices  $W^1, W^2, \dots, W^t$ 
2: while loss keeps improving do
3:   Sample  $\{m_{s,i}^l\}_{l \in \{1, \dots, t-1\}, s \in \{1, \dots, n\}, i \in \{1, \dots, N_l\}}$ 
4:   /* Execute local SGD's */
5:   for each site  $s$  do
6:     /* Send weights to local SGD */
7:     for each layer  $l$  do
8:       Compute  $\mathcal{W}_s^l = \{W_{i,j}^l\}_{s.t. m_{s,i}^l = 1, m_{s,j}^{l-1} = 1}$ 
9:       Send  $\mathcal{W}_s^l$  to site  $s$ 
10:    end for
11:    Run subnet local SGD at site  $s$ 
12:  end for
13:  /* Retrieve results of local SGD */
14:  for each site  $s$ , layer  $l$  do
15:    Retrieve updated  $\mathcal{W}_s^l$  from site  $s$ 
16:    for each  $(i, j)$  s.t.  $m_{s,i}^l = 1, m_{s,j}^{l-1} = 1$  do
17:      Update  $W^l$  by replacing  $W_{i,j}^l$  with corresponding value from
18:         $\mathcal{W}_s^l$ 
19:    end for
20:  end for
21: end while
    
```

Algorithm 2 IST local SGD.

Require: subnet s : $\mathcal{W}_s^1, \mathcal{W}_s^2, \mathcal{W}_s^3, \dots$, loss $\ell^{(i)}(\cdot)$, # of local iters. J , learning rate η , local batch size B

```

1: Let  $\mathcal{W}^{(0)} = \langle \mathcal{W}_s^1, \mathcal{W}_s^2, \mathcal{W}_s^3, \dots \rangle$ 
2: for  $t = 1, \dots, J$  do
3:   Let  $\mathcal{B}$  be a set of  $B$  samples from local data.
4:    $\mathcal{W}^{(t)} = \mathcal{W}^{(t-1)} - \eta \cdot \nabla \ell_{\mathcal{B}}(\mathcal{W}^{(t-1)})$ .
5: end for
6: Let  $\langle \mathcal{W}_s^1, \mathcal{W}_s^2, \mathcal{W}_s^3, \dots \rangle = \mathcal{W}^{(J)}$ 
7: Send  $\langle \mathcal{W}_s^1, \mathcal{W}_s^2, \mathcal{W}_s^3, \dots \rangle$  to coordinator
    
```

is an unbiased estimator for $W^l f^{l-1}$. Thus, it holds that $\hat{f}^l = f(n^2 \sum_s m_s^l \odot (W^l (m_s^{l-1} \odot \hat{f}^{l-1})))$ is a reasonable estimator for

$f^l = f(W^l f^{l-1})$. In doing so, we are guilty of applying a form of the classical statistical fallacy that for random variable x , if $\mathbb{E}[x] = b$, then $\mathbb{E}[f(x)] \approx f(b)$.

This fallacy is dangerous when the activation f is non-linear. Because the membership indicators force subsampling the inputs to each neuron (and a scale factor of n^2 is then applied to the resulting quantity to unbiased it), we end up increasing the standard deviation of the input to each neuron by a factor of n during training, compared to the standard deviation that will be observed during inference, without the use of membership indicators. This increased variance means that we are more likely to observe extreme inputs to each neuron during training than during actual deployment. The network learns to expect such extreme values and avoid saturation during deployment, and adapts accordingly. However, the learned network fails when it is deployed.

To match the training and deployment distributions, we could apply an analytic approach. Instead, we simply remove the n^2 correction. I.e., during training, for a given neuron, we compute the mean μ and standard deviation σ of the inputs to the neuron, and use a modified activation function $f'(x) = f((x - \mu)/\sigma)$. Before inference, we can compute μ and σ for each neuron over a small subset of the training data using the full network, and use those values during deployment.

Note that this is similar to batch normalization [28]—we can learn a scale and shift as well. Though our motivation for its use is somewhat different. Classically, batch normalization keeps the input in the non-saturated range of the activation function during training. This tends to speed convergence and improve generalization. Yet, IST *will simply not work* without some sort of normalization, due to the distributional shift that will be encountered when deploying the whole network.

3.4 Why Is This Fast?

By subsampling, we reduce both network traffic and compute workload. In addition, IST allows for periods of local updates with no communication, again reducing network traffic.

For a feed-forward NN, at each round of “classical” data parallel training, the entire set of parameters must be broadcast to each site. Measuring the inflow to each site, the total network traffic per gradient step is (in floating point numbers transferred): $\sum_{i=1}^l nN_{i-1}N_i$. In contrast, during IST, each site receives the current parameters only one time every J gradient steps. Subsampling reduces this cost further; the matrices attached to the input and output layers are partitioned across nodes (not broadcast), and only a $\frac{1}{n}$ fraction of the weights in each of the other matrices are sent to any node. The total network traffic per gradient step is: $\frac{N_0N_1+N_{l-1}N_l}{J} + \sum_{i=1}^l \frac{N_{i-1}N_i}{n \times J}$.

Computational resource utilization is reduced similarly. Considering the FLOPs required by matrix multiplications during forward and backward steps, during “classical” data parallel training, the number of FLOPs required per gradient step is: $4 \sum_{i=1}^l BN_{i-1}N_i$. In contrast, the number of FLOPs per IST gradient step is: $4BN_0N_1 + 4BN_{l-1}N_l + 4B \sum_{i=1}^l \frac{N_{i-1}N_i}{n}$. Note that this also explains the reduction of RAM usage for IST, which enables training of larger models.

In Figure 2 we plot the average cost of each gradient step as a function of the number of machines, assuming a feed forward NN

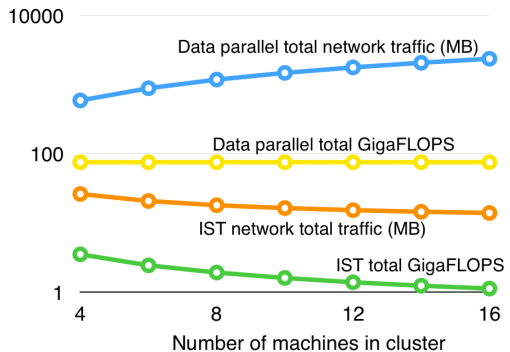


Figure 2: Comparing the cost of IST with data parallel learning.

with three hidden layers of 4,000 neurons, an input feature vector of 1,000 features, a batch size of 512 data objects, and 200 output labels, assuming J , the number of subnet local SGD steps, is 10. There is a radical decrease in both network traffic and FLOPS using IST. In particular, using IST both of these quantities *decrease* with the addition of more machines in the cluster.

Note that this plot does not tell the whole story, as IST may have lower (or higher) statistical efficiency. The fact that IST partitions the network and runs local updates may decrease efficiency, whereas the fact that each “batch” processed during IST actually consists of n independent samples of size B (compared to a single global sample in classical data parallel training) may tend to increase efficiency. This will be examined experimentally.

3.5 IST for other Architectures

As described, IST applies to fully-connected layers. Extending the method to other common neural constructs, such as convolutional layers, is straightforward. There are two ways that the IST decomposition can be used with a convolutional neural network (CNN).

The first and most straightforward way to do is to apply IST only to the fully-connected layer(s) that make part of nearly every modern CNN architecture. The fully-connected layers are decomposed as described in this paper, but, during training, the rest of the network is broadcast to every site. Even this simple decomposition has significant benefits as the fully-connected layer(s) tend to be the most expensive to move between sites during training. Consider the full ImageNet [34] for a deep model as ResNet50: the convolutional layers have 17,614,016 parameters (67.2MB, 28.2%), whereas the fully-connected layer at the top has 44,730,368 parameters (170.6MB, 71.8%) amenable to IST. In the experimental section of the paper, we show that this simple extension results in significant speedup of training VGG over the full ImageNet dataset.

A second and almost-as-straightforward way of applying IST to a CNN architecture is to partition the convolutional filters, by assigning non-overlapping subsets of filters to each of the machines in the compute cluster. We explicitly adopt this natural extension to basic residual blocks in Resnet, where the intermediate activations are partitioned by filter channels. In the experimental section of the paper, we show empirically that this natural extension can effectively lead to speedup in training Resnet over the CFAR10 data set.

Google Speech 2 Layer									
	Data Parallel			Local SGD			IST		
Accuracy	2 Node	4 Node	8 Node	2 Node	4 Node	8 Node	2 Node	4 Node	8 Node
0.63	118	269	450	68	130	235	35	28	24
0.75	759	1708	2417	444	742	1110	231	167	192
Google Speech 3 Layer									
	Data Parallel			Local SGD			IST		
Accuracy	2 Node	4 Node	8 Node	2 Node	4 Node	8 Node	2 Node	4 Node	8 Node
0.63	376	1228	1922	182	586	1115	76	141	300
0.75	4534	9340	14886	2032	4107	6539	812	664	1161
CIFAR10 Resnet18									
	Data Parallel			Local SGD			IST		
Accuracy	2 Node	4 Node	8 Node	2 Node	4 Node	8 Node	2 Node	4 Node	8 Node
0.85	21775	13689	6890	18769	12744	7020	15093	7852	5241
0.90	54002	38430	17853	36891	22198	12157	33345	16798	13425
Full ImageNet VGG12									
	Data Parallel			Local SGD			IST		
Accuracy	2 Node	4 Node	8 Node	2 Node	4 Node	8 Node	2 Node	4 Node	8 Node
0.20	108040	278542	504805	6900	14698	30441	3629	4379	5954
0.26	225911	393279	637188	15053	22055	39439	6189	7711	10622

Table 1: The time (in seconds) to reach various levels of accuracy.

3.6 Convergence of IST

It is possible to provide convergence guarantees for IST. Formal guarantees are provided in the Appendix of the paper. Since a proof of these guarantees is quite involved, we leave the full proof to in the appendix.

4 EMPIRICAL EVALUATION

In this section, we design a set of experiments designed to show the potential benefit of the IST approach when the goal is distributed training in a public cloud, with a relatively slow network but where fast CPUs and GPUs are available. To do this, we compare IST with data parallel learning and local SGD [37], on a variety of learning tasks and neural architectures.

Learning tasks and environment. (1) *Google Speech Commands* [54]: We learn a 2-layer network of 4096 neurons and a 3-layer network of 8192 neurons to recognize 35 labeled keywords from audio waveforms (in contrast to the 12 keywords in prior reports [54]). We represent each waveform as a 4096-dimensional feature vector [52]. (2) *Image classification on CIFAR10 and full ImageNet* [26, 49]: We train the Resnet18 model over CIFAR10, and the VGG12 model over full ImageNet (see Section 3.5 for a discussion of IST and non-fully connected architectures). **Note that we include the complete ImageNet dataset with all 21,841 categories and report the top-10 accuracy.** Because it is so difficult to train, there are few reported results over the complete ImageNet data set. (3) *Amazon-670k* [8]: We train a 2-layer, fully-connected neural network, which accepts a 135,909-dimensional input feature, and generates a prediction over 670,091 output labels. Further details of the learning tasks and hyperparameter tuning description are enumerated in the full version of the paper.

We train Google speech and Resnet18 on CIFAR10 on three AWS CPU clusters, with 2, 4, and 8 CPU instances (m5.2xlarge). We

train the VGG model on full ImageNet and Amazon-670k extreme classification network on three AWS GPU clusters, with 2, 4, and 8 GPU machines (p3.2xlarge). Our choice of AWS was deliberate, as it is a very common learning platform, and *illustrates the challenge faced by many consumers*: distributed ML without a super-fast interconnect.

Distributed Implementation Notes. We implement a distributed parameter server for IST in PyTorch. We compare IST to the PyTorch implementation of data parallel learning. We also adapt the PyTorch data parallel learning to realize local SGD [37], where learning occurs locally for a number of iterations before synchronizing.

For the CPU experiments, we use PyTorch’s `gloo` backend. For the GPU experiments, data parallel learning and local SGD use PyTorch’s `nccl` backend, which leverages the most advanced Nvidia collective communication library (the set of high-performance multi-GPU and multi-node collective communication primitives optimized for NVIDIA GPUs). `Nccl` implements ring-based all-reduce [1], which is used in well-known distributed learning systems such as Horovod [48].

Unfortunately, IST cannot use the `nccl` backend: it does not support the `scatter` operator required to implement IST, likely because the deep learning community has focused on data parallel learning. As a result, IST must use the `gloo` backend (meant for CPU-based learning). *This is a serious handicap for IST*, though we emphasize that it is not the result of any intrinsic flaw of the method, it is merely a lack of support for required operations in the high-performance GPU library.

The experimental results are summarized below:

Scalability. We first investigate the relative scaling of IST compared to the alternatives, with an increasing number of EC2 workers. For various configurations we time how long each of the distributed

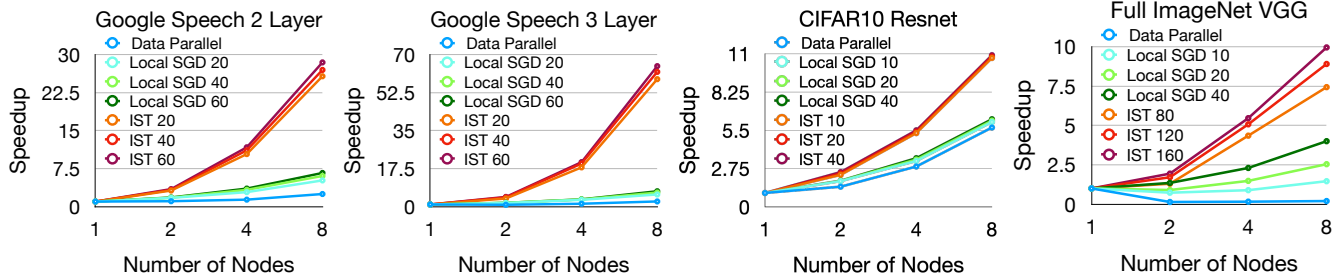


Figure 3: Scaling comparison of data parallel, local SGD and IST with various local update iterations. The speedup is calculated by comparing with the training time for one epoch to 1-worker SGD. The number after local SGD or IST legend represents the local update iterations.

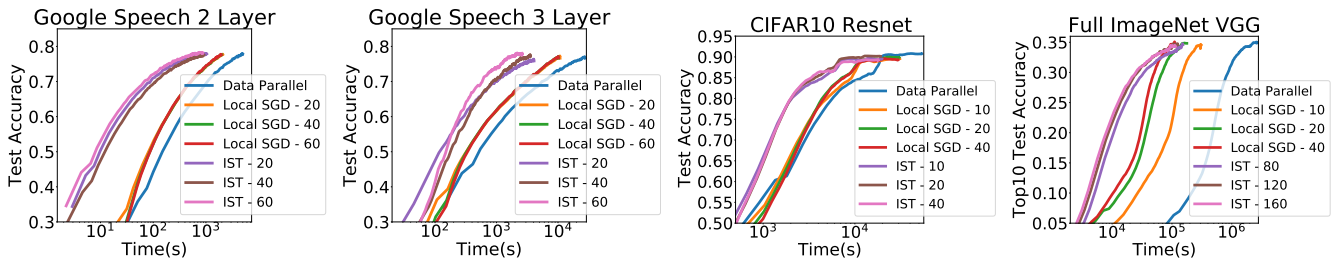


Figure 4: Test accuracy vs. time. 2-/3- layer Google speech models are trained using an 8-CPU cluster; Resnet18 on CIFAR10 is trained using 4-CPU cluster; VGG12 on full ImageNet is trained using a 8-GPU cluster. The number after local SGD or IST legend represents the local update iterations.

learning frameworks take to complete one training epoch. Figure 3 gives the results.

Convergence speed. While IST can process data quickly, there are questions regarding its statistical efficiency vis-a-vis the other methods, and how this affects convergence. Figure 4 plots the hold-out test accuracy for selected benchmarks as a function of time. Table 1 shows the training time required for the various methods to reach specified levels of hold-out test accuracy.

Trained model accuracy. Because IST is inherently a model-parallel training method, it has certain advantages, including the ability to scale to large models. We study the relationship between the embedding dimensions and the hold-out test performance for the Amazon-670k recommendation task in a 8-GPU cluster. The precision @1, @3, and @5 are reported in Table 2. In Table 3 we give the final accuracy of each method, trained on a 2-node cluster.

Discussion. There are a few takeaways from the experimental results. First, as expected, there are significant advantages to IST in terms of being able to process data quickly. Figure 3 shows that IST is able to process far more data in a short amount of time than the other distributed training algorithm. Interestingly, we find that the IST speedups in CPU clusters are more significant than that in GPU clusters. There are two reasons for this. First, for GPU clusters, IST suffers from its use of PyTorch’s `glow` backend, compared to the `all-reduce` operator provided by `nccl`. Second, since the GPU provides a very high level of computation, there is less benefit to be realized from the reduction in FLOPS per gradient step using IST (as the GPU does not appear to be compute bound).

Figure 4 and Table 1 generally show that IST is much faster compared to the other frameworks for achieving high levels of accuracy on a hold-out test set. For example, IST exhibits a 4.2 \times speedup compared to local SGD, and 10.6 \times speedup compared to classical data parallel for the 2-layer Google speech model to reach 77%. IST exhibits 6.1 \times speedup compared to local SGD, and a 16.6 \times speedup comparing to data parallel for the 3-layer model to reach the accuracy of 77%. Note that this was observed even though IST was handicapped by its use of `glow` for its GPU implementation. Interestingly, for the full ImageNet data set, the communication bottleneck using AWS is so severe that the smaller clusters were always faster; at each cluster size, IST was still the fastest option. For CFAR10, because CPUs were used for training, the network is less of a bottleneck and all methods were able to scale. This negates the IST advantage just a bit. In this case, IST was fastest to 85% accuracy, but was slower to fine-tune to 90% accuracy in 8-CPU cluster.

Dim	Data Parallel			IST		
	P@1	P@3	P@5	P@1	P@3	P@5
512	0.3861	0.3454	0.3164	0.3962	0.3604	0.3313
1024	Fail			0.4089	0.3685	0.3392
1536	Fail			0.4320	0.3907	0.3614
2048	Fail			0.4365	0.3936	0.3637
2560	Fail			0.4384	0.3944	0.3658

Table 2: Precision @1, @3, @5 on the Amazon 670k benchmark.

Another key advantage of IST is illustrated in Table 2; because it is a model-parallel framework and distributes the model to multiple

machines, IST is able to scale to virtually unlimited model sizes. In this case, it can compute 2560-dimensional embedding in 8-GPU cluster (and realize the associated, additional accuracy) whereas the data parallel approaches are unable to do this.

	Data Parallel	Local SGD	IST
Speech 2 layer	0.7938	0.7998	0.8153
Speech 3 layer	0.7950	0.7992	0.8327
CIFAR10 Resnet18	0.9128	0.9087	0.9102
Full Imagenet VGG12	0.3688	0.3685	0.3802

Table 3: Final accuracy on each benchmark.

It is interesting that *some of the frameworks actually do worse with additional machines, especially with a fast GPU*. This illustrates a significant problem with distributed learning. Unless a super-fast interconnect is used (and such interconnects are not available from typical cloud providers), it can actually be *detrimental* to add additional machines, as the added cost of transferring data can actually result in *slower* running times. We see this clearly in Table 1, where the state-of-the-art PyTorch data parallel implementation (and the local SGD variant) does significantly *worse* with more machines. IST shows the best potential to utilize additional machines without actually becoming much slower or slower to reach high accuracy.

Finally, we note that various compression schemes can be used to increase the bandwidth of the interconnect (e.g., gradient sparsification [3], quantization [4], sketching [29], and low-rank compression [53]). However, these methods could be used with *any* framework—including IST. We conjecture that while compression may allow effective scaling to larger clusters, it would not affect the efficacy of IST.

5 RELATED WORK

Data parallelism often suffers from the high bandwidth costs to communicate gradient updates between workers. Quantized SGD [4, 14, 17, 24, 27, 47, 55] and sparsified SGD [3] both address this. Quantized SGD uses lossy compression to quantize the gradients. Sparsified SGD reduces the exchange overhead by transmitting the gradients with maximal magnitude. Such methods are orthogonal to IST, and could be used in combination with it.

Recently, there has been a series of papers on using parallelism to “Solve the YY learning problem in XX minutes”, for ever-decreasing values of XX [13, 23, 50, 58, 60–62]. Often these methods employ large batches. It is generally accepted—though still debated [18]—that large batch training converges to “sharp minima”, hurting generalization [16, 31, 59]. Further, achieving such results seems to require teams of PhDs utilizing special-purpose hardware: there is no approach that generalizes well without extensive trial-and-error.

Distributed local SGD [40, 64, 65, 68] updates the parameters, through averaging, only after several local steps are performed per compute node. This reduces synchronization and thus allows for higher hardware efficiency [65]. IST uses a similar approach but makes the local SGD and each synchronization round less expensive. Recent approaches [37] propose less frequent synchronization towards the end of the training, but they cannot avoid it at the beginning.

Finally, asynchrony avoids SGD synchronization cost [15, 41, 45, 66]. It has been used in distributed-memory systems, such as

DistBelief [15] and the Project Adam [33]. While such systems, asymptotically, show nice convergence rate guarantees, there seems to be growing agreement that *unconstrained* asynchrony does not always work well [11], and it seems to be losing favor in practice.

6 CONCLUSION

In this work, we propose *independent subnet training* for distributed training of neural networks. By stochastically partitioning the model into non-overlapping subnets, IST reduces the communication overhead for model synchronization, and the computation workload of forward-backward propagation for a thinner model on each worker. This results in two advances: *i*) IST significantly accelerates the training process comparing with standard data parallel approaches for distributed learning, and *ii*) IST scales to large models that cannot be learned using standard data parallel approaches.

A CONVERGENCE GUARANTEES FOR IST

We will discuss the convergence behavior of IST in this section.

Consider the problem of minimizing an average of loss functions:

$$x^* \in \arg \min_{x \in \mathbb{R}^P} \left\{ f(x) := \frac{1}{n} \sum_{i=1}^n f_i(x) \right\}.$$

Here, $f_i(\cdot)$ denotes the contribution to the loss of the i -th data point. The components $f_i(\cdot)$ define the nature of the full function f : if f_i ’s are quadratics, we obtain the convex linear regression problem; if f_i ’s model the forward pass of a neural network, we obtain neural network inference.

In this note, we will consider f_i functions that do not follow exactly the architecture of a specific neural network, but satisfy general loss assumptions that could potentially be satisfied by neural network models.

ASSUMPTION 1. (L_i -smoothness) Given component f_i of f function, there exists constant $L_i > 0$ such that for every $x, y \in \mathbb{R}^P$ we have that:

$$\|\nabla f_i(x) - \nabla f_i(y)\|_2 \leq L_i \cdot \|x - y\|_2$$

or, equivalently,

$$f_i(y) \leq f_i(x) + \langle \nabla f_i(x), y - x \rangle + \frac{L_i}{2} \|x - y\|_2^2.$$

Further, define $L_{\max} := \max_i L_i$.

Another assumption that we use in part of our results is Q -Lipschitz assumption:

ASSUMPTION 2. (Q -Lipschitz continuity) Given f function, there exists constant $Q > 0$ such that for every $x, y \in \mathbb{R}^P$ we have that:

$$|f(x) - f(y)| \leq Q \cdot \|x - y\|_2$$

or, equivalently,

$$\|\nabla f(x)\|_2 \leq Q, \quad \forall x \in \mathbb{R}^P.$$

Two other assumptions for f functions that do not imply convexity but help as proof convergence rate techniques are:

ASSUMPTION 3. (Error Bound) Let x^* denote the global optimum of f . Then, under the Error Bound assumption, there exists constant $\mu > 0$ such that for every $x \in \mathbb{R}^P$ we have that:

$$\|\nabla f(x)\|_2 \geq \mu \|x^* - x\|_2$$

Per [30], Error Bound \equiv Polyak-Lojasiewicz inequality.

Regarding stochasticity in gradient descent, we will use the following general assumptions on the boundedness of stochastic gradient variance.

ASSUMPTION 4. (Stochastic gradient variance) We assume that there are constants $M, M_f > 0$, such that

$$\mathbb{E}_{i_t} [\|\nabla f_{i_t}(x)\|_2^2] \leq M + M_f \|\nabla f(x)\|_2^2,$$

where f_{i_t} is a randomly selected component from the sum $\frac{1}{n} \sum_{i=1}^n f_i(x)$.

For the rest of the text, we make the distinction between the general indexing term i and the randomly selected index per SGD round, i_t . The differences are clear from the context.

A.1 Compressed iterates

We follow the problem formulation in [32] on compressed iterates. Working on IST in a sequentially centralized fashion, IST performs the following motions:

- Given current model x_t at iteration t , we generate a mask $\mathcal{M} : \mathbb{R}^P \rightarrow \mathbb{R}^P$ such that:

$$(\mathcal{M}(x_t))_i = \begin{cases} \frac{x_{t,i}}{\xi}, & \text{with probability } \xi, \\ 0, & \text{with probability } 1 - \xi. \end{cases}$$

This mask deviates from the proposed model in the sense that the input and output neurons in the neural network are always selected.

- Given mask $\mathcal{M}(\cdot)$, we generate the subnetwork as in:

$$y_t \equiv \mathcal{M}(x_t) \in \mathbb{R}^P,$$

where y_t has zeros at the positions where neurons are deactivated for this subnetwork at iteration t and non-zeros for the active weights. I.e., y_t constitutes a *compressed* version of the full model x_t .

- We perform gradient descent on the compressed y_t as in:

$$x_{t+1} = y_t - \eta \nabla f_{i_t}(y_t),$$

for η being the learning rate, and i_t being selected randomly from $[n]$.

The above setting resembles that of *gradient descent with compressed iterates* (GD CI) in [32]. Our analysis differentiates in that we consider a different function class.

Compression operators $\mathcal{M}(\cdot)$ Let us describe and prove some properties of the compression operator $\mathcal{M}(\cdot)$.

PROPERTY 1. (Unbiasedness of $\mathcal{M}(\cdot)$) The operator $\mathcal{M} : \mathbb{R}^P \rightarrow \mathbb{R}^P$ as defined above is unbiased; i.e.,

$$\mathbb{E}_{\mathcal{M}} [\mathcal{M}(x) | x] = x, \quad \forall x \in \mathbb{R}^P$$

PROOF. To see this, we compute:

$$\begin{aligned} \mathbb{E}_{\mathcal{M}} [\mathcal{M}(x) | x] &= \begin{bmatrix} \mathbb{E}_{\mathcal{M}} [(\mathcal{M}(x))_1 | x] \\ \mathbb{E}_{\mathcal{M}} [(\mathcal{M}(x))_2 | x] \\ \vdots \\ \mathbb{E}_{\mathcal{M}} [(\mathcal{M}(x))_p | x] \end{bmatrix} \\ &= \begin{bmatrix} \xi \cdot \frac{x_1}{\xi} + (1 - \xi) \cdot 0 \\ \xi \cdot \frac{x_2}{\xi} + (1 - \xi) \cdot 0 \\ \vdots \\ \xi \cdot \frac{x_p}{\xi} + (1 - \xi) \cdot 0 \end{bmatrix} = \begin{bmatrix} x_1 \\ x_2 \\ \vdots \\ x_p \end{bmatrix} = x \end{aligned}$$

□

PROPERTY 2. (Bounded variance of $\mathcal{M}(\cdot)$) The operator $\mathcal{M} : \mathbb{R}^P \rightarrow \mathbb{R}^P$ has bounded variance as in:

$$\mathbb{E}_{\mathcal{M}} [\|\mathcal{M}(x) - x\|_2^2 | x] = \frac{1 - \xi}{\xi} \|x\|_2^2, \quad \forall x \in \mathbb{R}^P$$

PROOF. Let us first expand the squared term:

$$\begin{aligned} &\mathbb{E}_{\mathcal{M}} [\|\mathcal{M}(x) - x\|_2^2 | x] \\ &= \mathbb{E}_{\mathcal{M}} [\|\mathcal{M}(x)\|_2^2 + \|x\|_2^2 - 2\langle \mathcal{M}(x), x \rangle | x] \\ &= \mathbb{E}_{\mathcal{M}} [\|\mathcal{M}(x)\|_2^2 | x] + \|x\|_2^2 - 2\langle \mathbb{E}_{\mathcal{M}} [\mathcal{M}(x) | x], x \rangle \\ &= \mathbb{E}_{\mathcal{M}} [\|\mathcal{M}(x)\|_2^2 | x] - \|x\|_2^2 \end{aligned}$$

Focusing on the first term on the right hand side:

$$\begin{aligned} &\mathbb{E}_{\mathcal{M}} [\|\mathcal{M}(x)\|_2^2 | x] \\ &= \mathbb{E}_{\mathcal{M}} \left[\sum_{i=1}^p (\mathcal{M}(x))_i^2 | x \right] = \sum_{i=1}^p \mathbb{E}_{\mathcal{M}} [(\mathcal{M}(x))_i^2 | x] \\ &= \sum_{i=1}^p \left(\xi \cdot \frac{x_i^2}{\xi^2} + (1 - \xi) \cdot 0 \right) = \frac{1}{\xi} \sum_{i=1}^p x_i^2 = \frac{1}{\xi} \|x\|_2^2 \end{aligned}$$

Combining the above we get:

$$\mathbb{E}_{\mathcal{M}} [\|\mathcal{M}(x) - x\|_2^2 | x] = \frac{1}{\xi} \|x\|_2^2 - \|x\|_2^2 = \frac{1 - \xi}{\xi} \|x\|_2^2$$

□

Some assumptions we make for $\mathcal{M}(\cdot)$ with regard to the gradient of f are as follows.

ASSUMPTION 5. (Additive gradient error assumption with bounded energy) Let x_t be the current model and let $y_t = \mathcal{M}(x_t)$ be the compressed model. Consider the stochastic gradient term $\nabla f_{i_t}(y_t)$; we assume that, on expectation, the following additive noise assumption holds:

$$\begin{aligned} &\mathbb{E}_{\mathcal{M}, i_t} [\nabla f_{i_t}(y_t) | x_t] = \nabla f(x_t) + \varepsilon_t, \\ &\text{for } \varepsilon_t \in \mathbb{R}^P \text{ such that } \|\varepsilon_t\|_2 \leq B \text{ for } B > 0. \end{aligned}$$

A different assumption that can be made for stochastic gradient $\nabla f_{i_t}(y_t)$ is the *norm condition*, used in derivative free optimization [5, 10]:

ASSUMPTION 6. (Norm condition) There is a constant $\theta \in [0, 1)$ such that:

$$\|\mathbb{E}_{\mathcal{M}, i_t} [\nabla f_{i_t}(y_t) | x_t] - \nabla f(x_t)\|_2 = \|\varepsilon_t\|_2 \leq \theta \|\nabla f(x_t)\|_2,$$

where x_t is the current model and $y_t = \mathcal{M}(x_t)$ is the compressed model.

A.2 Proof of sequential IST

In this subsection, we will provide the backbone of our proof; later on we will make different assumptions that will lead to different final results. For this first part, we will only use the basic properties of the compression operator $\mathcal{M}(\cdot)$ and the L -smoothness of f .

We start with the following Lemma.

LEMMA 1. *Let $y_t = \mathcal{M}(x_t)$. Then, for x^\star the optimal point for f , it holds:*

$$\mathbb{E}_{\mathcal{M}} [\|y_t - x_t\|_2^2 \mid x_t] \leq \frac{2(1-\xi)}{\xi} \|x_t - x^\star\|_2^2 + \frac{2(1-\xi)}{\xi} \|x^\star\|_2^2.$$

PROOF. By Property 2, we know that:

$$\mathbb{E}_{\mathcal{M}} [\|y_t - x_t\|_2^2 \mid x_t] = \frac{1-\xi}{\xi} \|x_t\|_2^2.$$

Combining this with the property that:

$$\|x_t\|_2^2 = \|x_t - x^\star + x^\star\|_2^2 \leq 2\|x_t - x^\star\|_2^2 + 2\|x^\star\|_2^2,$$

we get the reported result. \square

Moreover, we also state the following Lemma, which is used in most proofs below.

LEMMA 2. *Let $y_t = \mathcal{M}(x_t)$. Then,*

$$\begin{aligned} & \mathbb{E}_{\mathcal{M}, i_t} [\|y_t - x_t - \eta \nabla f_{i_t}(y_t)\|_2^2 \mid x_t] \\ & \leq \frac{4(1+\eta^2 L_{\max}^2)(1-\xi)}{\xi} (\|x_t - x^\star\|_2^2 + \|x^\star\|_2^2) + 2\eta^2 \mathbb{E}_{i_t} [\|\nabla f_{i_t}(x_t)\|_2^2 \mid x_t]. \end{aligned}$$

PROOF. For any $z \in \mathbb{R}^p$, we have:

$$\begin{aligned} & \mathbb{E}_{\mathcal{M}, i_t} [\|y_t - x_t - \eta \nabla f_{i_t}(y_t)\|_2^2 \mid x_t] \\ & = \mathbb{E}_{\mathcal{M}, i_t} [\|y_t - x_t - \eta \nabla f_{i_t}(z) + \eta \nabla f_{i_t}(z) - \eta \nabla f_{i_t}(y_t)\|_2^2 \mid x_t] \\ & \leq 2 \cdot \mathbb{E}_{\mathcal{M}, i_t} [\|y_t - x_t - \eta \nabla f_{i_t}(z)\|_2^2 \mid x_t] \\ & \quad + 2\eta^2 \cdot \mathbb{E}_{\mathcal{M}, i_t} [\|\nabla f_{i_t}(z) - \nabla f_{i_t}(y_t)\|_2^2 \mid x_t] \\ & = 2 \cdot \mathbb{E}_{\mathcal{M}, i_t} [\|y_t - x_t\|_2^2 + \eta^2 \|\nabla f_{i_t}(z)\|_2^2 - 2\eta \cdot \langle \nabla f_{i_t}(z), y_t - x_t \rangle \mid x_t] \\ & \quad + 2\eta^2 \cdot \mathbb{E}_{\mathcal{M}, i_t} [\|\nabla f_{i_t}(z) - \nabla f_{i_t}(y_t)\|_2^2 \mid x_t] \end{aligned}$$

Observe that

$$\begin{aligned} \mathbb{E}_{\mathcal{M}, i_t} [\langle \nabla f_{i_t}(z), y_t - x_t \rangle \mid x_t] & = \langle \mathbb{E}_{i_t} [\nabla f_{i_t}(z)], \mathbb{E}_{\mathcal{M}} [y_t \mid x_t] - x_t \rangle \\ & = \langle \nabla f(z), x_t - x_t \rangle = 0 \end{aligned}$$

due to Property 1. Then:

$$\begin{aligned} & \mathbb{E}_{\mathcal{M}, i_t} [\|y_t - x_t - \eta \nabla f(y_t)\|_2^2 \mid x_t] \\ & \leq 2 \cdot \mathbb{E}_{\mathcal{M}} [\|y_t - x_t\|_2^2 \mid x_t] + 2\eta^2 \mathbb{E}_{i_t} [\|\nabla f_{i_t}(z)\|_2^2 \mid x_t] \\ & \quad + 2\eta^2 \cdot \mathbb{E}_{\mathcal{M}, i_t} [\|\nabla f_{i_t}(z) - \nabla f_{i_t}(y_t)\|_2^2 \mid x_t] \end{aligned}$$

By L_i -smoothness, we have:

$$\begin{aligned} & \mathbb{E}_{\mathcal{M}, i_t} [\|\nabla f(z) - \nabla f(y_t)\|_2^2 \mid x_t] \\ & \leq \mathbb{E}_{\mathcal{M}, i_t} [L_{i_t}^2 \cdot \|z - y_t\|_2^2 \mid x_t] \\ & \leq L_{\max}^2 \cdot \mathbb{E}_{\mathcal{M}, i_t} [\|z - y_t\|_2^2 \mid x_t] \\ & \leq L_{\max}^2 \cdot \mathbb{E}_{\mathcal{M}} [\|z - x_t + x_t - y_t\|_2^2 \mid x_t] \\ & = L_{\max}^2 \cdot \mathbb{E}_{\mathcal{M}} [\|z - x_t\|_2^2 + \|x_t - y_t\|_2^2 + 2\langle z - x_t, x_t - y_t \rangle \mid x_t] \\ & = L_{\max}^2 \cdot \mathbb{E}_{\mathcal{M}} [\|z - x_t\|_2^2 \mid x_t] + L_{\max}^2 \cdot \mathbb{E}_{\mathcal{M}} [\|x_t - y_t\|_2^2 \mid x_t] \end{aligned}$$

In the above, we used Property 1 to get $\mathbb{E}_{\mathcal{M}} [y_t \mid x_t] = x_t$. Using this result in the expression above, we get:

$$\begin{aligned} & \mathbb{E}_{\mathcal{M}, i_t} [\|y_t - x_t - \eta \nabla f_{i_t}(y_t)\|_2^2 \mid x_t] \\ & \leq 2 \cdot \mathbb{E}_{\mathcal{M}} [\|y_t - x_t\|_2^2 \mid x_t] + 2\eta^2 \mathbb{E}_{i_t} [\|\nabla f_{i_t}(z)\|_2^2 \mid x_t] \\ & \quad + 2\eta^2 \cdot L_{\max}^2 \cdot (\mathbb{E}_{\mathcal{M}} [\|z - x_t\|_2^2 \mid x_t] + \mathbb{E}_{\mathcal{M}} [\|x_t - y_t\|_2^2 \mid x_t]) \\ & = 2(1 + \eta^2 L_{\max}^2) \cdot \mathbb{E}_{\mathcal{M}} [\|y_t - x_t\|_2^2 \mid x_t] + 2\eta^2 \mathbb{E}_{i_t} [\|\nabla f_{i_t}(z)\|_2^2 \mid x_t] \\ & \quad + 2\eta^2 \cdot L_{\max}^2 \cdot \mathbb{E}_{\mathcal{M}} [\|z - x_t\|_2^2 \mid x_t] \end{aligned}$$

The above expression holds for any $z \in \mathbb{R}^p$, and thus it will hold for $z = x_t$. In this case, the above inequality becomes:

$$\begin{aligned} & \mathbb{E}_{\mathcal{M}, i_t} [\|y_t - x_t - \eta \nabla f_{i_t}(y_t)\|_2^2 \mid x_t] \\ & \leq 2(1 + \eta^2 L_{\max}^2) \cdot \mathbb{E}_{\mathcal{M}} [\|y_t - x_t\|_2^2 \mid x_t] + 2\eta^2 \mathbb{E}_{i_t} [\|\nabla f_{i_t}(x_t)\|_2^2 \mid x_t] \end{aligned}$$

Finally, using Lemma 1, we obtain the desired inequality. \square

The following lemma leads to a general recursion over function values, that will lead to specific convergence rate guarantees later on, based on additional assumptions.

LEMMA 3. *Let f be L -smooth, and consider the recursion over compressed iterates:*

$$x_{t+1} = y_t - \eta \nabla f_{i_t}(y_t), \quad \text{where } y_t = \mathcal{M}(x_t).$$

Then the following recursion holds:

$$\begin{aligned} \mathbb{E}_{\mathcal{M}, i_t} [f(x_{t+1}) \mid x_t] & \leq f(x_t) - \eta \cdot \langle \nabla f(x_t), \mathbb{E}_{\mathcal{M}, i_t} [\nabla f_{i_t}(y_t) \mid x_t] \rangle \\ & \quad + \frac{L_t}{2} \cdot \mathbb{E}_{\mathcal{M}, i_t} [\|y_t - \eta \nabla f_{i_t}(y_t) - x_t\|_2^2 \mid x_t], \end{aligned}$$

where the expectation is over the random selection on the compression operator $\mathcal{M}(\cdot)$ and the stochasticity of the gradient.

PROOF. Starting from the L_i -smoothness condition, we have on expectation with respect to \mathcal{M}, i_t at time t :

$$\begin{aligned}
 & \mathbb{E}_{\mathcal{M}, i_t} [f(x_{t+1}) \mid x_t] \\
 & \leq \mathbb{E}_{\mathcal{M}, i_t} \left[f(x_t) + \langle \nabla f_i(x_t), x_{t+1} - x_t \rangle + \frac{L_i}{2} \|x_{t+1} - x_t\|_2^2 \mid x_t \right] \\
 & = \mathbb{E}_{\mathcal{M}, i_t} [f(x_t) \mid x_t] + \mathbb{E}_{\mathcal{M}, i_t} [\langle \nabla f_i(x_t), x_{t+1} - x_t \rangle \mid x_t] \\
 & \quad + \frac{L_i}{2} \cdot \mathbb{E}_{\mathcal{M}, i_t} [\|x_{t+1} - x_t\|_2^2 \mid x_t] \\
 & = f(x_t) + \mathbb{E}_{\mathcal{M}, i_t} [\langle \nabla f_i(x_t), y_t - \eta \nabla f_i(y_t) - x_t \rangle \mid x_t] \\
 & \quad + \frac{L_i}{2} \cdot \mathbb{E}_{\mathcal{M}, i_t} [\|y_t - \eta \nabla f_i(y_t) - x_t\|_2^2 \mid x_t] \\
 & = f(x_t) + \mathbb{E}_{\mathcal{M}, i_t} [\langle \nabla f_i(x_t), y_t - x_t \rangle \mid x_t] \\
 & \quad - \eta \cdot \mathbb{E}_{\mathcal{M}, i_t} [\langle \nabla f_i(x_t), \nabla f_i(y_t) \rangle \mid x_t] \\
 & \quad + \frac{L_i}{2} \cdot \mathbb{E}_{\mathcal{M}, i_t} [\|y_t - \eta \nabla f(y_t) - x_t\|_2^2 \mid x_t] \\
 & = f(x_t) + \langle \mathbb{E}_{i_t} [\nabla f_i(x_t) \mid x_t], \mathbb{E}_{\mathcal{M}} [y_t \mid x_t] - x_t \rangle \\
 & \quad - \eta \cdot \langle \mathbb{E}_{i_t} [\nabla f_i(x_t) \mid x_t], \mathbb{E}_{\mathcal{M}, i_t} [\nabla f_i(y_t) \mid x_t] \rangle \\
 & \quad + \frac{L_i}{2} \cdot \mathbb{E}_{\mathcal{M}, i_t} [\|y_t - \eta \nabla f_i(y_t) - x_t\|_2^2 \mid x_t] \\
 & \stackrel{\text{Property 1}}{=} f(x_t) - \eta \cdot \langle \nabla f(x_t), \mathbb{E}_{\mathcal{M}, i_t} [\nabla f_i(y_t) \mid x_t] \rangle \\
 & \quad + \frac{L_i}{2} \cdot \mathbb{E}_{\mathcal{M}, i_t} [\|y_t - \eta \nabla f_i(y_t) - x_t\|_2^2 \mid x_t]
 \end{aligned}$$

In the last step, we also used the unbiasedness of the stochastic gradient. \square

Our proof will branch out for different assumptions we make. We begin with the following ‘‘cocktail’’ of assumptions.

THEOREM 1. *Let $f := \frac{1}{n} \sum_{i=1}^n f_i(x)$ has L_i -smooth components f_i for $L_{\max} := \max_i L_i$, and consider the recursion over compressed iterates:*

$$x_{t+1} = y_t - \eta \nabla f_i(y_t), \quad \text{where } y_t = \mathcal{M}(x_t).$$

In addition to Lemma 3, we further assume that f is Q -Lipschitz, and satisfies the Error Bound with parameter $\mu > 0$. Further, our recursion should satisfy the gradient boundedness Assumption 4 for $M > 0$ and $0 < M_f < 1$. Finally, we assume that the operator mask, along with f , satisfy the additive gradient error assumption with bounded energy such that:

$$\begin{aligned}
 & \mathbb{E}_{\mathcal{M}, i_t} [\nabla f_i(y_t) \mid x_t] = \nabla f(x_t) + \varepsilon_t, \\
 & \text{for } \varepsilon_t \in \mathbb{R}^p \text{ such that } \|\varepsilon_t\|_2 \leq B \text{ for } B > 0.
 \end{aligned}$$

Then, after running the above recursion for T iterations for step size $\eta = \frac{1}{2L_{\max}}$, we obtain:

$$\begin{aligned}
 & \min_{t \in \{0, \dots, T\}} \mathbb{E}_{\mathcal{M}, i_t} [\|\nabla f(x_t)\|_2^2] \\
 & \leq \frac{f(x_0) - f(x^*)}{\alpha(T+1)} + \frac{1}{\alpha} \cdot \left(\frac{BQ}{2L_{\max}} + \frac{5L_{\max}\omega}{2} \cdot \|x^*\|_2^2 + \frac{M}{4L_{\max}} \right)
 \end{aligned}$$

where the expectation is over the random selection on the compression operator $\mathcal{M}(\cdot)$ and the stochastic selection i_t , $\alpha = \frac{1}{2L_{\max}} \left(1 - \frac{M_f}{2}\right) - \frac{5\omega L_{\max}}{2\mu^2}$, and $\omega = \frac{1-\xi}{\xi} < \frac{\mu^2}{10L_{\max}^2}$.

PROOF. We know from Lemma 3 that the following holds:

$$\begin{aligned}
 \mathbb{E}_{\mathcal{M}, i_t} [f(x_{t+1}) \mid x_t] & \leq f(x_t) - \eta \cdot \langle \nabla f(x_t), \mathbb{E}_{\mathcal{M}, i_t} [\nabla f_i(y_t) \mid x_t] \rangle \\
 & \quad + \frac{L_i}{2} \cdot \mathbb{E}_{\mathcal{M}, i_t} [\|y_t - \eta \nabla f_i(y_t) - x_t\|_2^2 \mid x_t],
 \end{aligned}$$

Using the additive gradient noise assumption $\mathbb{E}_{\mathcal{M}, i_t} [\nabla f_i(y_t) \mid x_t] = \nabla f(x_t) + \varepsilon_t$, we have:

$$\begin{aligned}
 & \mathbb{E}_{\mathcal{M}, i_t} [f(x_{t+1}) \mid x_t] \\
 & \leq f(x_t) - \eta \cdot \langle \nabla f(x_t), \nabla f(x_t) \rangle \\
 & \quad + \varepsilon_t + \frac{L_i}{2} \cdot \mathbb{E}_{\mathcal{M}, i_t} [\|y_t - \eta \nabla f_i(y_t) - x_t\|_2^2 \mid x_t] \\
 & = f(x_t) - \eta \cdot \|\nabla f(x_t)\|_2^2 - \eta \langle \nabla f(x_t), \varepsilon_t \rangle \\
 & \quad + \frac{L_i}{2} \cdot \mathbb{E}_{\mathcal{M}, i_t} [\|y_t - \eta \nabla f_i(y_t) - x_t\|_2^2 \mid x_t] \\
 & \stackrel{\text{Lemma 2}}{\leq} f(x_t) - \eta \cdot \|\nabla f(x_t)\|_2^2 - \eta \langle \nabla f(x_t), \varepsilon_t \rangle \\
 & \quad + \frac{L_i}{2} \cdot \left(\frac{4(1+\eta^2 L_{\max}^2)(1-\xi)}{\xi} (\|x_t - x^*\|_2^2 + \|x^*\|_2^2) + 2\eta^2 \mathbb{E}_{i_t} [\|\nabla f_i(x_t)\|_2^2 \mid x_t] \right) \\
 & \stackrel{L_i \leq L_{\max}}{\leq} f(x_t) - \eta \cdot \|\nabla f(x_t)\|_2^2 - \eta \langle \nabla f(x_t), \varepsilon_t \rangle \\
 & \quad + \frac{L_{\max}}{2} \cdot \left(\frac{4(1+\eta^2 L_{\max}^2)(1-\xi)}{\xi} (\|x_t - x^*\|_2^2 + \|x^*\|_2^2) + 2\eta^2 \mathbb{E}_{i_t} [\|\nabla f_i(x_t)\|_2^2 \mid x_t] \right) \\
 & \stackrel{\text{Assumption 4}}{\leq} f(x_t) - \eta \cdot \|\nabla f(x_t)\|_2^2 - \eta \langle \nabla f(x_t), \varepsilon_t \rangle \\
 & \quad + \frac{L_{\max}}{2} \cdot \left(\frac{4(1+\eta^2 L_{\max}^2)(1-\xi)}{\xi} (\|x_t - x^*\|_2^2 + \|x^*\|_2^2) + 2\eta^2 (M + M_f \|\nabla f(x_t)\|_2^2) \right) \\
 & = f(x_t) - \eta(1 - \eta L_{\max} M_f) \cdot \|\nabla f(x_t)\|_2^2 - \eta \langle \nabla f(x_t), \varepsilon_t \rangle \\
 & \quad + \frac{2L_{\max}(1+\eta^2 L_{\max}^2)(1-\xi)}{\xi} (\|x_t - x^*\|_2^2 + \|x^*\|_2^2) + L_{\max} \eta^2 M \\
 & \stackrel{\text{Error Bound}}{\leq} f(x_t) - \eta(1 - \eta L_{\max} M_f) \cdot \|\nabla f(x_t)\|_2^2 - \eta \langle \nabla f(x_t), \varepsilon_t \rangle \\
 & \quad + \frac{2L_{\max}(1+\eta^2 L_{\max}^2)(1-\xi)}{\xi} \cdot \frac{1}{\mu^2} \cdot \|\nabla f(x_t)\|_2^2 \\
 & \quad + \frac{2L_{\max}(1+\eta^2 L_{\max}^2)(1-\xi)}{\xi} \|x^*\|_2^2 + L_{\max} \eta^2 M
 \end{aligned}$$

To simplify notation, define $\omega = \frac{1-\xi}{\xi}$. Rearranging the terms in the inequality above we obtain:

$$\begin{aligned}
 & \mathbb{E}_{\mathcal{M}, i_t} [f(x_{t+1}) \mid x_t] \\
 & \leq f(x_t) - \left(\eta(1 - \eta L_{\max} M_f) - 2L_{\max}(1 + \eta^2 L_{\max}^2) \cdot \frac{\omega}{\mu^2} \right) \cdot \|\nabla f(x_t)\|_2^2 \\
 & \quad - \eta \langle \nabla f(x_t), \varepsilon_t \rangle + 2\omega L_{\max}(1 + \eta^2 L_{\max}^2) \|x^*\|_2^2 + L_{\max} \eta^2 M
 \end{aligned}$$

Define $g(\eta) = \eta(1 - \eta L_{\max} M_f) - 2L_{\max}(1 + \eta^2 L_{\max}^2) \cdot \frac{\omega}{\mu^2}$ which is a quadratic function. We set the step size as in $\eta = \frac{1}{2L_{\max}}$, which is a reasonable assumption based on convex optimization criteria. Then,

$$g\left(\frac{1}{2L_{\max}}\right) = \frac{1}{2L_{\max}} \left(1 - \frac{M_f}{2}\right) - \frac{5L_{\max}\omega}{2\mu^2} \equiv \alpha.$$

For the proof, we require $\alpha > 0$; according to our assumptions, $1 - \frac{M_f}{2} > \frac{1}{2} \Rightarrow M_f < 1$. This further leads to the requirement that

$\frac{1-\xi}{\xi} < \frac{\mu^2}{10L_{\max}^2}$. The above result into:

$$\begin{aligned}
 & \mathbb{E}_{\mathcal{M},i_t} [f(x_{t+1}) \mid x_t] \\
 & \leq f(x_t) - \alpha \cdot \|\nabla f(x_t)\|_2^2 - \eta \langle \nabla f(x_t), \varepsilon_t \rangle \\
 & \quad + 2\omega L_{\max}(1 + \eta^2 L_{\max}^2) \|x^*\|_2^2 + L_{\max} \eta^2 M \\
 \text{Cauchy-Schwarz} \\
 & \leq f(x_t) - \alpha \cdot \|\nabla f(x_t)\|_2^2 + \eta \cdot \|\nabla f(x_t)\|_2 \cdot \|\varepsilon_t\|_2 \\
 & \quad + 2\omega L_{\max}(1 + \eta^2 L_{\max}^2) \|x^*\|_2^2 + L_{\max} \eta^2 M \\
 \eta = \frac{1}{2L_{\max}} \\
 & = f(x_t) - \alpha \cdot \|\nabla f(x_t)\|_2^2 + \frac{1}{2L_{\max}} \cdot \|\nabla f(x_t)\|_2 \cdot \|\varepsilon_t\|_2 \\
 & \quad + \frac{5L_{\max}\omega}{2} \cdot \|x^*\|_2^2 + \frac{M}{4L_{\max}} \\
 \text{Q-Lipschitz} \\
 & \leq f(x_t) - \alpha \cdot \|\nabla f(x_t)\|_2^2 + \frac{Q}{2L_{\max}} \cdot \|\varepsilon_t\|_2 \\
 & \quad + \frac{5L_{\max}\omega}{2} \cdot \|x^*\|_2^2 + \frac{M}{4L_{\max}} \\
 \|\varepsilon_t\|_2 \leq B \\
 & \leq f(x_t) - \alpha \cdot \|\nabla f(x_t)\|_2^2 + \frac{BQ}{2L_{\max}} + \frac{5L_{\max}\omega}{2} \cdot \|x^*\|_2^2 + \frac{M}{4L_{\max}}
 \end{aligned}$$

Using the law of total expectation $\mathbb{E}[X] = \mathbb{E}[\mathbb{E}[X \mid Y]]$, we have:

$$\mathbb{E}[f(x_{t+1})] = \mathbb{E}[\mathbb{E}[f(x_{t+1}) \mid x_t]]$$

and thus:

$$\begin{aligned}
 \mathbb{E}_{\mathcal{M},i_t} [f(x_{t+1})] & \leq \mathbb{E}_{\mathcal{M},i_t} [f(x_t)] - \alpha \cdot \mathbb{E}_{\mathcal{M},i_t} [\|\nabla f(x_t)\|_2^2] \\
 & \quad + \frac{BQ}{2L} + \frac{5L_{\max}\omega}{2} \cdot \|x^*\|_2^2 + \frac{M}{4L_{\max}}
 \end{aligned}$$

Using the fact that $f(x^*) \leq \mathbb{E}_{\mathcal{M},i_t} [f(x_{T+1})]$, and telescoping over T iterations, we obtain:

$$\begin{aligned}
 f(x^*) & \leq \mathbb{E}_{\mathcal{M},i_t} [f(x_{T+1})] \\
 & \leq f(x_0) - \alpha \sum_{t=0}^T \mathbb{E}_{\mathcal{M},i_t} [\|\nabla f(x_t)\|_2^2] \\
 & \quad + (T+1) \cdot \left(\frac{BQ}{2L} + \frac{5L_{\max}\omega}{2} \cdot \|x^*\|_2^2 + \frac{M}{4L_{\max}} \right)
 \end{aligned}$$

which further leads to:

$$\begin{aligned}
 & \sum_{t=0}^T \mathbb{E}_{\mathcal{M},i_t} [\|\nabla f(x_t)\|_2^2] \\
 & \leq \frac{f(x_0) - f(x^*)}{\alpha} + \frac{T+1}{\alpha} \cdot \left(\frac{BQ}{2L} + \frac{5L_{\max}\omega}{2} \cdot \|x^*\|_2^2 + \frac{M}{4L_{\max}} \right)
 \end{aligned}$$

Observe that: $(T+1) \cdot \min_{t \in \{0, \dots, T\}} \mathbb{E}_{\mathcal{M},i_t} [\|\nabla f(x_t)\|_2^2] \leq \sum_{t=0}^T \mathbb{E}_{\mathcal{M},i_t} [\|\nabla f(x_t)\|_2^2]$, which leads to the final result:

$$\begin{aligned}
 & \min_{t \in \{0, \dots, T\}} \mathbb{E}_{\mathcal{M},i_t} [\|\nabla f(x_t)\|_2^2] \\
 & \leq \frac{f(x_0) - f(x^*)}{\alpha(T+1)} + \frac{1}{\alpha} \cdot \left(\frac{BQ}{2L} + \frac{5L_{\max}\omega}{2} \cdot \|x^*\|_2^2 + \frac{M}{4L_{\max}} \right)
 \end{aligned}$$

□

In the following corollary, we exchange the bounded assumption $\|\varepsilon_t\|_2 \leq B$ and Q -Lipschitzness, with the norm condition in Assumption 6.

COROLLARY 1. *Let f be L -smooth, and consider the recursion over compressed iterates:*

$$x_{t+1} = y_t - \eta \nabla f_{i_t}(y_t), \quad \text{where } y_t = \mathcal{M}(x_t).$$

In addition to Lemma 3, we further assume that the operator mask, along with f , satisfy the norm condition Assumption 6 with parameter

$\theta \in [0, 1)$. Then, after running the above recursion for T iterations for step size $\eta = \frac{1}{2L_{\max}}$, we obtain:

$$\min_{t \in \{0, \dots, T\}} \mathbb{E}_{\mathcal{M},i_t} [\|\nabla f(x_t)\|_2^2] \leq \frac{f(x_0) - f(x^*)}{\alpha(T+1)} + \frac{1}{\alpha} \cdot \left(\frac{5L_{\max}\omega}{2} \cdot \|x^*\|_2^2 + \frac{M}{4L_{\max}} \right)$$

where the expectation is over the random selection on the compression operator $\mathcal{M}(\cdot)$, $\alpha = \frac{1}{2L_{\max}} \left(\frac{1}{2} - \theta - \frac{M_f}{2} \right) - \frac{5L_{\max}}{2} \cdot \frac{\omega}{\mu^2}$, and $\omega = \frac{1-\xi}{\xi} < \frac{\mu^2}{5L_{\max}^2 \left(\frac{1}{2} - \theta - \frac{M_f}{2} \right)}$.

PROOF. From Theorem 1, we have:

$$\begin{aligned}
 & \mathbb{E}_{\mathcal{M},i_t} [f(x_{t+1}) \mid x_t] \\
 & \leq f(x_t) - \left(\eta(1 - \eta L_{\max} M_f) - 2L_{\max}(1 + \eta^2 L_{\max}^2) \cdot \frac{\omega}{\mu^2} \right) \cdot \|\nabla f(x_t)\|_2^2 \\
 & \quad - \eta \langle \nabla f(x_t), \mathbb{E}_{\mathcal{M},i_t} [\varepsilon_t \mid x_t] \rangle + 2\omega L_{\max}(1 + \eta^2 L_{\max}^2) \|x^*\|_2^2 + L_{\max} \eta^2 M \\
 \text{Cauchy-Schwarz} \\
 & \leq f(x_t) - \left(\eta(1 - \eta L_{\max} M_f) - 2L_{\max}(1 + \eta^2 L_{\max}^2) \cdot \frac{\omega}{\mu^2} \right) \cdot \|\nabla f(x_t)\|_2^2 \\
 & \quad + \eta \|\nabla f(x_t)\|_2 \cdot \|\mathbb{E}_{\mathcal{M},i_t} [\varepsilon_t \mid x_t]\|_2 + 2\omega L_{\max}(1 + \eta^2 L_{\max}^2) \|x^*\|_2^2 + L_{\max} \eta^2 M \\
 & = f(x_t) - \left(\eta(1 - \eta L_{\max} M_f) - 2L_{\max}(1 + \eta^2 L_{\max}^2) \cdot \frac{\omega}{\mu^2} \right) \cdot \|\nabla f(x_t)\|_2^2 \\
 & \quad + \eta \|\nabla f(x_t)\|_2 \cdot \|\mathbb{E}_{\mathcal{M},i_t} [\nabla f_{i_t}(y_t) \mid x_t] - \nabla f(x_t)\|_2 \\
 & \quad + 2\omega L_{\max}(1 + \eta^2 L_{\max}^2) \|x^*\|_2^2 + L_{\max} \eta^2 M \\
 \text{Norm condition} \\
 & \leq f(x_t) - \left(\eta(1 - \eta L_{\max} M_f) - 2L_{\max}(1 + \eta^2 L_{\max}^2) \cdot \frac{\omega}{\mu^2} \right) \cdot \|\nabla f(x_t)\|_2^2 \\
 & \quad + \eta \theta \|\nabla f(x_t)\|_2^2 + 2\omega L_{\max}(1 + \eta^2 L_{\max}^2) \|x^*\|_2^2 + L_{\max} \eta^2 M \\
 & = f(x_t) - \left(\eta(1 - \theta - \eta L_{\max} M_f) - 2L_{\max}(1 + \eta^2 L_{\max}^2) \cdot \frac{\omega}{\mu^2} \right) \cdot \|\nabla f(x_t)\|_2^2 \\
 & \quad + 2\omega L_{\max}(1 + \eta^2 L_{\max}^2) \|x^*\|_2^2 + L_{\max} \eta^2 M
 \end{aligned}$$

For coherence, assume that $\eta = \frac{1}{2L_{\max}}$. Following the same procedure we obtain, we define $g\left(\frac{1}{2L_{\max}}\right) \equiv \alpha = \frac{1}{2L_{\max}} \left(\frac{1}{2} - \theta - \frac{M_f}{2} \right) - \frac{5L_{\max}}{2} \cdot \frac{\omega}{\mu^2}$. We observe that $\alpha > 0$ when $\omega < \frac{\mu^2}{5L_{\max}^2 \left(\frac{1}{2} - \theta - \frac{M_f}{2} \right)}$. Then,

with similar reasoning with Theorem 1, we telescope the inequality to obtain:

$$\begin{aligned}
 & \min_{t \in \{0, \dots, T\}} \mathbb{E}_{\mathcal{M},i_t} [\|\nabla f(x_t)\|_2^2] \\
 & \leq \frac{f(x_0) - f(x^*)}{\alpha(T+1)} + \frac{1}{\alpha} \cdot \left(\frac{5L_{\max}\omega}{2} \cdot \|x^*\|_2^2 + \frac{M}{4L_{\max}} \right)
 \end{aligned}$$

□

REFERENCES

- [1] 2018. NCCL BASED MULTI-GPU TRAINING. <http://on-demand.gputechconf.com/gtc-cn/2018/pdf/CH8209.pdf>. Accessed: 2020-02-06.
- [2] Martin Abadi, Paul Barham, Jianmin Chen, Zhifeng Chen, Andy Davis, Jeffrey Dean, Matthieu Devin, Sanjay Ghemawat, Geoffrey Irving, Michael Isard, et al. 2016. Tensorflow: A system for large-scale machine learning. In *12th {USENIX} Symposium on Operating Systems Design and Implementation ({OSDI} 16)*. 265–283.
- [3] Alham Fikri Aji and Kenneth Heafield. 2017. Sparse communication for distributed gradient descent. *arXiv preprint arXiv:1704.05021* (2017).
- [4] Dan Alistarh, Demjan Grubic, Jerry Li, Ryota Tomioka, and Milan Vojnovic. 2017. QSGD: Communication-efficient SGD via gradient quantization and encoding. In *Advances in Neural Information Processing Systems*. 1709–1720.
- [5] A. Berahas, L. Cao, K. Choromanski, and K. Scheinberg. 2019. A theoretical and empirical comparison of gradient approximations in derivative-free optimization. *arXiv preprint arXiv:1905.01332* (2019).

- [6] Albert S Berahas, Raghu Bollapragada, and Jorge Nocedal. 2017. An investigation of Newton-sketch and subsampled Newton methods. *arXiv preprint arXiv:1705.06211* (2017).
- [7] Albert S Berahas, Majid Jahani, and Martin Takáč. 2019. Quasi-Newton Methods for Deep Learning: Forget the Past, Just Sample. *arXiv preprint arXiv:1901.09997* (2019).
- [8] Kush Bhatia, Kunal Dahiya, Himanshu Jain, Yashoteja Prabhu, and Manik Varma. [n.d.]. *The Extreme Classification Repository: Multi-label Datasets and Code*. <http://manikvarma.org/downloads/XC/XMLRepository.html>.
- [9] Léon Bottou, Frank E Curtis, and Jorge Nocedal. 2018. Optimization methods for large-scale machine learning. *Siam Review* 60, 2 (2018), 223–311.
- [10] R. Carter. 1991. On the global convergence of trust region algorithms using inexact gradient information. *SIAM J. Numer. Anal.* 28, 1 (1991), 251–265.
- [11] Jianmin Chen, Xinghao Pan, Rajat Monga, Samy Bengio, and Rafal Jozefowicz. 2016. Revisiting distributed synchronous SGD. *arXiv preprint arXiv:1604.00981* (2016).
- [12] Trishul M Chilimbi, Yutaka Suzue, Johnson Apacible, and Karthik Kalyanaraman. 2014. Project Adam: Building an Efficient and Scalable Deep Learning Training System. In *OSDI*, Vol. 14. 571–582.
- [13] Valeriu Codreanu, Damian Podareanu, and Vikram Saletore. 2017. Scale out for large minibatch SGD: Residual network training on ImageNet-1K with improved accuracy and reduced time to train. *arXiv preprint arXiv:1711.04291* (2017).
- [14] Matthieu Courbariaux, Yoshua Bengio, and Jean-Pierre David. 2015. BinaryConnect: Training deep neural networks with binary weights during propagations. In *Advances in neural information processing systems*. 3123–3131.
- [15] Jeffrey Dean, Greg Corrado, Rajat Monga, Kai Chen, Matthieu Devin, Mark Mao, Andrew Senior, Paul Tucker, Ke Yang, Quoc V Le, et al. 2012. Large scale distributed deep networks. In *Advances in neural information processing systems*. 1223–1231.
- [16] Aaron Defazio and Léon Bottou. 2018. On the Ineffectiveness of Variance Reduced Optimization for Deep Learning. *arXiv preprint arXiv:1812.04529* (2018).
- [17] Tim Dettmers. 2015. 8-bit approximations for parallelism in deep learning. *arXiv preprint arXiv:1511.04561* (2015).
- [18] Laurent Dinh, Razvan Pascanu, Samy Bengio, and Yoshua Bengio. 2017. Sharp minima can generalize for deep nets. In *Proceedings of the 34th International Conference on Machine Learning-Volume 70*. JMLR.org, 1019–1028.
- [19] Petros Drineas, Ravi Kannan, and Michael W Mahoney. 2006. Fast Monte Carlo algorithms for matrices I: Approximating matrix multiplication. *SIAM J. Comput.* 36, 1 (2006), 132–157.
- [20] John Duchi, Elad Hazan, and Yoram Singer. 2011. Adaptive subgradient methods for online learning and stochastic optimization. *Journal of Machine Learning Research* 12, Jul (2011), 2121–2159.
- [21] Philipp Farber and Krste Asanovic. 1997. Parallel neural network training on multi-processor. In *Algorithms and Architectures for Parallel Processing, 1997. ICAPP 97, 1997 3rd International Conference on*. IEEE, 659–666.
- [22] Noah Golmant, Nikita Vemuri, Zhewei Yao, Vladimir Feinberg, Amir Gholami, Kai Rothauge, Michael W Mahoney, and Joseph Gonzalez. 2018. On the Computational Inefficiency of Large Batch Sizes for Stochastic Gradient Descent. *arXiv preprint arXiv:1811.12941* (2018).
- [23] Priya Goyal, Piotr Dollár, Ross Girshick, Pieter Noordhuis, Lukasz Wesolowski, Aapo Kyrola, Andrew Tulloch, Yangqing Jia, and Kaiming He. 2017. Accurate, large minibatch SGD: training ImageNet in 1 hour. *arXiv preprint arXiv:1706.02677* (2017).
- [24] Suyog Gupta, Ankur Agrawal, Kailash Gopalakrishnan, and Pritish Narayanan. 2015. Deep learning with limited numerical precision. In *International Conference on Machine Learning*. 1737–1746.
- [25] Stefan Hadjis, Ce Zhang, Ioannis Mitliagkas, Dan Iter, and Christopher Ré. 2016. Omnivore: An optimizer for multi-device deep learning on CPUs and GPUs. *arXiv preprint arXiv:1606.04487* (2016).
- [26] Kaiming He, Xiangyu Zhang, Shaoqing Ren, and Jian Sun. 2016. Deep residual learning for image recognition. In *Proceedings of the IEEE conference on computer vision and pattern recognition*. 770–778.
- [27] Itay Hubara, Matthieu Courbariaux, Daniel Soudry, Ran El-Yaniv, and Yoshua Bengio. 2017. Quantized Neural Networks: Training Neural Networks with Low Precision Weights and Activations. *Journal of Machine Learning Research* 18, 187 (2017), 1–30.
- [28] Sergey Ioffe and Christian Szegedy. 2015. Batch Normalization: Accelerating Deep Network Training by Reducing Internal Covariate Shift. In *International Conference on Machine Learning*. 448–456.
- [29] Nikita Iykin, Daniel Rothchild, Enayat Ullah, Ion Stoica, Raman Arora, et al. 2019. Communication-efficient distributed sgd with sketching. In *Advances in Neural Information Processing Systems*. 13144–13154.
- [30] H. Karimi, J. Nutini, and M. Schmidt. 2016. Linear convergence of gradient and proximal-gradient methods under the Polyak-Łojasiewicz condition. In *Joint European Conference on Machine Learning and Knowledge Discovery in Databases*. Springer, 795–811.
- [31] Nitish Shirish Keskar, Dheevatsa Mudigere, Jorge Nocedal, Mikhail Smolyanskiy, and Ping Tak Peter Tang. 2016. On large-batch training for deep learning: Generalization gap and sharp minima. *arXiv preprint arXiv:1609.04836* (2016).
- [32] A. Khaled and P. Richtárik. 2019. Gradient descent with compressed iterates. *arXiv preprint arXiv:1909.04716* (2019).
- [33] Diederik P Kingma and Jimmy Ba. 2014. Adam: A method for stochastic optimization. *arXiv preprint arXiv:1412.6980* (2014).
- [34] A. Krizhevsky, I. Sutskever, and G. Hinton. 2012. Imagenet classification with deep convolutional neural networks. In *Advances in neural information processing systems*. 1097–1105.
- [35] Sudhir B Kylasa, Farbod Roosta-Khorasani, Michael W Mahoney, and Ananth Grama. 2018. GPU Accelerated Sub-Sampled Newton’s Method. *arXiv preprint arXiv:1802.09113* (2018).
- [36] Mu Li, David G Andersen, Jun Woo Park, Alexander J Smola, Amr Ahmed, Vanja Josifovski, James Long, Eugene J Shekita, and Bor-Yiing Su. 2014. Scaling Distributed Machine Learning with the Parameter Server. In *OSDI*, Vol. 14. 583–598.
- [37] Tao Lin, Sebastian U Stich, and Martin Jaggi. 2018. Don’t Use Large Mini-Batches, Use Local SGD. *arXiv preprint arXiv:1808.07217* (2018).
- [38] Linjian Ma, Gabe Montague, Jiayu Ye, Zhewei Yao, Amir Gholami, Kurt Keutzer, and Michael W Mahoney. 2019. Inefficiency of K-FAC for Large Batch Size Training. *arXiv preprint arXiv:1903.06237* (2019).
- [39] James Martens and Roger Grosse. 2015. Optimizing neural networks with Kronecker-factored approximate curvature. In *International conference on machine learning*. 2408–2417.
- [40] Ryan McDonald, Mehryar Mohri, Nathan Silberman, Dan Walker, and Gideon S Mann. 2009. Efficient large-scale distributed training of conditional maximum entropy models. In *Advances in Neural Information Processing Systems*. 1231–1239.
- [41] Thomas Paine, Hailin Jin, Jianchao Yang, Zhe Lin, and Thomas Huang. 2013. GPU asynchronous stochastic gradient descent to speed up neural network training. *arXiv preprint arXiv:1312.6186* (2013).
- [42] Adam Paszke, Sam Gross, Soumith Chintala, Gregory Chanan, Edward Yang, Zachary DeVito, Zeming Lin, Alban Desmaison, Luca Antiga, and Adam Lerer. 2017. Automatic differentiation in pytorch. (2017).
- [43] Rajat Raina, Anand Madhavan, and Andrew Y Ng. 2009. Large-scale deep unsupervised learning using graphics processors. In *Proceedings of the 26th annual international conference on machine learning*. ACM, 873–880.
- [44] Alexander Ratner, Dan Alistarh, Gustavo Alonso, Peter Bailis, Sarah Bird, Nicholas Carlini, Bryan Catanzaro, Eric Chung, Bill Dally, Jeff Dean, et al. 2019. SysML: The New Frontier of Machine Learning Systems. *arXiv preprint arXiv:1904.03257* (2019).
- [45] Benjamin Recht, Christopher Re, Stephen Wright, and Feng Niu. 2011. Hogwild: A lock-free approach to parallelizing stochastic gradient descent. In *Advances in neural information processing systems*. 693–701.
- [46] Sebastian Ruder. 2016. An overview of gradient descent optimization algorithms. *arXiv preprint arXiv:1609.04747* (2016).
- [47] Frank Seide, Hao Fu, Jasha Droppo, Gang Li, and Dong Yu. 2014. 1-bit stochastic gradient descent and its application to data-parallel distributed training of speech DNNs. In *Fifteenth Annual Conference of the International Speech Communication Association*.
- [48] Alexander Sergeev and Mike Del Balso. 2018. Horovod: fast and easy distributed deep learning in TensorFlow. *arXiv preprint arXiv:1802.05799* (2018).
- [49] K. Simonyan and A. Zisserman. 2014. Very deep convolutional networks for large-scale image recognition. *arXiv preprint arXiv:1409.1556* (2014).
- [50] Samuel L Smith, Pieter-Jan Kindermans, Chris Ying, and Quoc V Le. 2017. Don’t decay the learning rate, increase the batch size. *arXiv preprint arXiv:1711.00489* (2017).
- [51] Nitish Srivastava, Geoffrey Hinton, Alex Krizhevsky, Ilya Sutskever, and Ruslan Salakhutdinov. 2014. Dropout: a simple way to prevent neural networks from overfitting. *The Journal of Machine Learning Research* 15, 1 (2014), 1929–1958.
- [52] Stanley Smith Stevens, John Volkman, and Edwin B Newman. 1937. A scale for the measurement of the psychological magnitude pitch. *The Journal of the Acoustical Society of America* 8, 3 (1937), 185–190.
- [53] Thijs Vogels, Sai Praneeth Karimireddy, and Martin Jaggi. 2019. PowerSGD: Practical low-rank gradient compression for distributed optimization. In *Advances in Neural Information Processing Systems*. 14236–14245.
- [54] Pete Warden. 2018. Speech commands: A dataset for limited-vocabulary speech recognition. *arXiv preprint arXiv:1804.03209* (2018).
- [55] Wei Wen, Cong Xu, Feng Yan, Chunpeng Wu, Yandan Wang, Yiran Chen, and Hai Li. 2017. Terngrad: Ternary gradients to reduce communication in distributed deep learning. In *Advances in neural information processing systems*. 1509–1519.
- [56] Stephen Wright and Jorge Nocedal. 1999. Numerical optimization. *Springer Science* 35, 67–68 (1999), 7.
- [57] Peng Xu, Farbod Roosta-Khorasani, and Michael W Mahoney. 2017. Newton-type methods for non-convex optimization under inexact hessian information. *arXiv preprint arXiv:1708.07164* (2017).
- [58] Omry Yadan, Keith Adams, Yaniv Taigman, and Marc’Aurelio Ranzato. 2013. Multi-GPU training of convnets. *arXiv preprint arXiv:1312.5853* (2013).
- [59] Zhewei Yao, Amir Gholami, Qi Lei, Kurt Keutzer, and Michael W Mahoney. 2018. Hessian-based analysis of large batch training and robustness to adversaries. In

- Advances in Neural Information Processing Systems*. 4949–4959.
- [60] Yang You, Igor Gitman, and Boris Ginsburg. 2017. Scaling SGD batch size to 32K for ImageNet training. *arXiv preprint arXiv:1708.03888* (2017).
- [61] Yang You, Jonathan Hseu, Chris Ying, James Demmel, Kurt Keutzer, and Cho-Jui Hsieh. 2019. Large-Batch Training for LSTM and Beyond. *arXiv preprint arXiv:1901.08256* (2019).
- [62] Yang You, Jing Li, Jonathan Hseu, Xiaodan Song, James Demmel, and Cho-Jui Hsieh. 2019. Reducing BERT Pre-Training Time from 3 Days to 76 Minutes. *arXiv preprint arXiv:1904.00962* (2019).
- [63] Matthew D Zeiler. 2012. ADADELTA: an adaptive learning rate method. *arXiv preprint arXiv:1212.5701* (2012).
- [64] Ce Zhang and Christopher Ré. 2014. Dimmwitted: A study of main-memory statistical analytics. *Proceedings of the VLDB Endowment* 7, 12 (2014), 1283–1294.
- [65] Jian Zhang, Christopher De Sa, Ioannis Mitliagkas, and Christopher Ré. 2016. Parallel SGD: When does averaging help? *arXiv preprint arXiv:1606.07365* (2016).
- [66] Shanshan Zhang, Ce Zhang, Zhao You, Rong Zheng, and Bo Xu. 2013. Asynchronous stochastic gradient descent for DNN training. In *Acoustics, Speech and Signal Processing (ICASSP), 2013 IEEE International Conference on*. IEEE, 6660–6663.
- [67] Xiru Zhang, Michael Mckenna, Jill P Mesirov, and David L Waltz. 1990. An efficient implementation of the back-propagation algorithm on the connection machine CM-2. In *Advances in neural information processing systems*. 801–809.
- [68] Martin Zinkevich, Markus Weimer, Lihong Li, and Alex J Smola. 2010. Parallelized stochastic gradient descent. In *Advances in neural information processing systems*. 2595–2603.